

The effects of collision energy and ion vibrational excitation on proton and charge transfer in $\text{H}_2^+ + \text{N}_2$, CO, O₂

S. L. Anderson, T. Turner, B. H. Mahan, and Y. T. Lee

Citation: *The Journal of Chemical Physics* **77**, 1842 (1982); doi: 10.1063/1.444036

View online: <http://dx.doi.org/10.1063/1.444036>

View Table of Contents: <http://scitation.aip.org/content/aip/journal/jcp/77/4?ver=pdfcov>

Published by the AIP Publishing

Articles you may be interested in

[Selective vibrational excitation and mode conservation in \$\text{H}^+ + \text{CO}_2/\text{N}_2\text{O}\$ inelastic and charge transfer collisions](#)
J. Chem. Phys. **87**, 2067 (1987); 10.1063/1.453182

[Energy and charge transfer in \$\text{O}^+ + 2\$ on \$\text{O}_2\$ collisions: Effects of a “vibrational rainbow”](#)
J. Chem. Phys. **83**, 5690 (1985); 10.1063/1.449643

[Charge transfer excitation in \$\text{Ne}^+ - \text{N}_2\text{O}\$ collisions at energies down to 1 eV](#)
J. Chem. Phys. **70**, 2030 (1979); 10.1063/1.437637

[Charge transfer and Penning ionization of \$\text{N}_2\$, CO, \$\text{CO}_2\$, and \$\text{H}_2\text{S}\$ in proton excited helium mixtures](#)
J. Chem. Phys. **67**, 3376 (1977); 10.1063/1.435284

[Charge transfer excitation channels in positive ion- \$\text{N}_2\text{O}\$ collisions at low energy](#)
J. Chem. Phys. **66**, 4111 (1977); 10.1063/1.434484



The effects of collision energy and ion vibrational excitation on proton and charge transfer in $\text{H}_2^+ + \text{N}_2$, CO , O_2

S. L. Anderson,^{a)} T. Turner,^{b)} B. H. Mahan, and Y. T. Lee^{c)}

Materials and Molecular Research Division, Lawrence Berkeley Laboratory and Department of Chemistry, University of California, Berkeley, California 94720

(Received 27 April 1982; accepted 14 May 1982)

The effects of vibrational excitation of reagent ions and collision energy on the proton and charge transfer reactions of H_2^+ and D_2^+ with N_2 , CO , and O_2 have been investigated using a method combining photoionization and a radio frequency guided ion technique. For proton transfer the $\text{H}_2^+ + \text{N}_2$ results are quite similar to the $\text{H}_2^+ + \text{Ar}$ system; proton and charge transfer channels are closely coupled for kinetic energies above 3 eV. In contrast, for $\text{H}_2^+ + \text{CO}$, the vibrational dependence of proton transfer is quite weak. For the $\text{H}_2^+ + \text{O}_2$ case, evidence is seen for direct competition between the charge and proton transfer process. A simple model for charge transfer is used to assess the importance of energy resonance and Franck-Condon effects. In these simple molecular systems, the energy defect is found to be most important to charge exchange, although Franck-Condon factors play a substantial role.

I. INTRODUCTION

The study of vibrational effects on reactivity and on the dynamics of reactions has been pursued for many years. In some neutral reactions where only one potential energy surface is involved, the observed effects are generally well understood. Using classical trajectory calculations, Polanyi and co-workers¹ have shown, e.g., that in reactions which have barriers in the exit channel (typical of endoergic reactions), vibrational motion increases the probability of surmounting the barrier. Experimental evidence² shows that at least near threshold, vibrational energy indeed is very effective in promoting endoergic reactions.

The effects of vibrational excitation on ion-molecule reactions are often more complicated than the enhancement of nuclear motion in overcoming the potential energy barriers. While many neutral reactions are governed by a single potential energy surface (PES), nearly all ion-molecule systems have at least two low lying potential energy surfaces corresponding to $A^+ + BC$ and $A + BC^+$ at large reagent distances. These surfaces have crossings and avoided crossings and, except for cases like $\text{H}_2^+ + \text{He}$ where the first excited PES lies far above the $\text{H}_2^+ + \text{He}$ ground PES, transitions between different surfaces and different electronic configurations of the systems during the collisions are likely. Taking the energetics of $(\text{H}_2 + \text{Ar})^+$ as an example, Fig. 1 schematically shows a cut along the BC stretch coordinate through the entrance channel of the PES for an $A^+ + BC$ collision. Here, A and BC have similar ionization potentials and two electronic states of the system ($A^+ + BC$ and $A + BC^+$) lie very close together. At infinite reagent separation [Fig. 1(a)], the two PES cross and there is no mixing between charge states. As the reagents come together, the two charge states which are of the same symmetry, begin to mix and the crossing becomes avoided. Initially, the inter-

action is weak and the motion of the system, including the BC vibration, remains on the diabatic $A^+ + BC$ potential surface [Fig. 1(b)]. As the reagent separation decreases, the mixing becomes stronger [Fig. 1(c)] and the splitting between the two new adiabatic surfaces created by the avoided crossing becomes larger. At this point, motion of the system through the avoided crossing seam (the surface of intersection between the two multidimensional PES's) can be either diabatic (retaining the same electronic configuration) or adiabatic (remaining on the same PES). This allows the possibility of transitions between the two reagent charge states and between the ground PES and the excited adiabatic PES. Figure 1(d) shows the potential curves when the reagents are close together. Here, the motion is strictly on a single PES, since the surface splitting is too large to allow transitions. Thus, as the reagents approach each other through the entrance channel, vibrational motion couples the two charge states and also can cause hopping to the excited PES. These electronic effects induced by the vibrational motion can far outweigh simple effects of enhanced nuclear motion in overcoming potential energy barriers. This vibrationally induced charge and/or surface hopping has been studied theoretically for the $\text{H}_2^+ + \text{H}_2$ system³ and for the $\text{Ar}^+ + \text{H}_2$ system.⁴

Recently, we have investigated the effects of vibration and collision energy on a number of simple ion-molecule reactions. In $\text{H}_2^+ + \text{H}_2$, we found a very complex pattern of collision and vibrational energy dependences for charge transfer, proton transfer, and collision induced dissociation.⁵ The data was interpreted in light of the calculated potential surfaces³ for $\text{H}_2^+ + \text{H}_2$ and provides strong evidence for the importance of avoided crossings in determining the dynamics of $\text{H}_2^+ + \text{H}_2$ collisions. In H_2^+ with Ar ,⁶ avoided crossings are again found to strongly influence the dynamics of both proton and charge transfers, although the dynamics of the proton transfer reaction appears to be more complicated than those suggested from the results of potential energy surface calculations.⁴ Coupling between the two charge states also seems to strongly influence the proton transfer reaction, especially at higher collision energies.

^{a)}National Science Foundation Graduate Fellow. Present address: Department of Chemistry, Stanford University, Stanford, California 94305.

^{b)}Fannie and John Hertz Graduate Fellow.

^{c)}Miller Professor, 1981-1982.

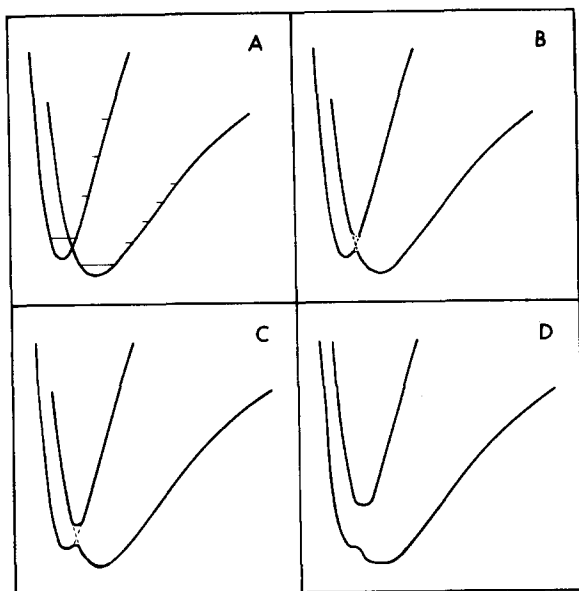


FIG. 1. Cuts through a typical ion-molecule reaction entrance channel. (a) Infinite reagent separation, (b) $R(\text{A}-\text{BC}) \equiv 5 \text{ \AA}$, (c) $R(\text{A}-\text{BC}) \equiv 3 \text{ \AA}$, (d) small reagent separation. Energetics are appropriate for $(\text{H}_2 + \text{Ar})^+$.

It is interesting to compare the dynamics of charge and proton transfer of H_2^+ with Ar^6 with the analogous reactions with N_2 , CO , and O_2 . The four systems are similar in some ways, but very different in others. The proton and charge transfer reactions (PT and CT) and their energetics, calculated from data in Ref. 7, are summarized in Table I. Since the N_2 , CO , and O_2 bonds are quite strong (they might be called pseudo-atoms), no other reactions occur in the collision energy range which our experiments cover, except for collision induced dissociation of H_2^+ (CID), which has a maximum cross section of less than 3 \AA^2 for all three systems and will not be considered here.

Examination of Table I shows that while all the PT reactions are substantially exoergic, there is a wide variation in the energetics of CT. In particular, both $\text{H}_2^+ + \text{Ar}$ and $\text{H}_2^+ + \text{N}_2$ are slightly endoergic, while both $\text{H}_2^+ + \text{CO}$ and $\text{H}_2^+ + \text{O}_2$ are quite exoergic. This would be expected to lead to large differences in the general shape of the PES's as well as on the magnitudes of the CT cross sections. The entrance channel of $\text{H}_2^+ + \text{N}_2$ will look very similar to that of $\text{H}_2^+ + \text{Ar}$ shown in Fig. 1. Figure 2 shows the similar cut through the PES entrance channel for the case where the IP of the molecule is substantially lower than that of H_2 , as in $\text{H}_2^+ + \text{CO}$. In this case, an avoided crossing would allow all H_2^+ vibrational states to charge transfer and we might expect to see very different vibrational effects on both the CT and PT reactions.

A large difference between Ar and N_2 , CO , or O_2 in the reactions with H_2^+ is that the diatomics contain additional vibrational and rotational degrees of freedom which increase the number of possible product states substantially. We saw in CT of $\text{H}_2^+ + \text{Ar}$ that one of the strongest influences on the observed vibrational effects

TABLE I. Energetics of the major reaction channels.

$\text{H}_2^+ + \text{H}_2 \rightarrow \text{N}_2^+(X^2\Sigma_g^+) + \text{H}_2$	$\Delta E = 0.155 \text{ eV}$
$\text{H}_2^+ + \text{N}_2 \rightarrow \text{N}_2^+(A_2^2) + \text{H}_2$	$\Delta E = 1.29 \text{ eV}$
$\text{H}_2^+ + \text{N}_2 \rightarrow \text{N}_2\text{H}^+ + \text{H}$	$\Delta E = -2.38 \text{ eV}$
$\text{H}_2^+ + \text{CO} \rightarrow \text{CO}^+(X^2\Sigma^+) + \text{H}_2$	$\Delta E = -1.41 \text{ eV}$
$\text{H}_2^+ + \text{CO} \rightarrow \text{CO}^+(A^2\Pi) + \text{H}_2$	$\Delta E = 1.16 \text{ eV}$
$\text{H}_2^+ + \text{CO} \rightarrow \text{HCO}^+ + \text{H}$	$\Delta E = -3.51 \text{ eV}$
$\text{H}_2^+ + \text{O}_2 \rightarrow \text{O}_2^+(X^2\Pi_g) + \text{H}_2$	$\Delta E = -3.35 \text{ eV}$
$\text{H}_2^+ + \text{O}_2 \rightarrow \text{O}_2^+(a^4\Pi_u) + \text{H}_2$	$\Delta E = 0.73 \text{ eV}$
$\text{H}_2^+ + \text{O}_2 \rightarrow \text{O}_2^+(A^2\Pi_u) + \text{H}_2$	$\Delta E = 1.69 \text{ eV}$
$\text{H}_2^+ + \text{O}_2 \rightarrow \text{O}_2\text{H}^+ + \text{H}$	$\Delta E = -1.69 \text{ eV}$
$\text{H}_2^+ + \text{Ar} \rightarrow \text{Ar}^+(^2P_{3/2}) + \text{H}_2$	$\Delta E = 0.33 \text{ eV}$
$\text{H}_2^+ + \text{Ar} \rightarrow \text{Ar}^+(^2P_{1/2}) + \text{H}_2$	$\Delta E = 0.51 \text{ eV}$
$\text{H}_2^+ + \text{Ar} \rightarrow \text{ArH}^+ + \text{H}$	$\Delta E = -1.30 \text{ eV}$

appeared to be energy resonances between the $\text{H}_2^+(v) + \text{Ar}$ initial states and the available final states.⁶ The differing number and energy spacings of the product states in $\text{H}_2^+ + \text{Ar}$, N_2 , CO , and O_2 provides very different patterns of energy resonances for these four systems. Since exoergic CT appears to occur through a long range interaction, one might also expect that, in addition to the energy resonances, the overlap between an initial state wave function and the various final states—some variety of Franck-Condon factor—would have a large effect on charge transfer probability for systems such as $\text{H}_2^+ + \text{N}_2$, CO , and O_2 .

Although the reaction dynamics of N_2^+ , CO^+ , and O_2^+ + H_2 have been investigated quite extensively, not a great deal is known about the reactions of $\text{H}_2^+ + \text{N}_2$, CO , and O_2 . Bowers *et al.*⁸ studied reactions in the $(\text{H}_2 + \text{N}_2)^+$ system at thermal energies using the ion cyclotron resonance (ICR) technique. They determined rate constants for N_2H^+ formation from both $\text{H}_2^+ + \text{N}_2$ and $\text{N}_2^+ + \text{H}_2$ (1.95 and $1.4 \times 10^{-9} \text{ cm}^3 \text{ molecule}^{-1} \text{ s}^{-1}$, respectively) and found that the $\text{H}_2^+ + \text{N}_2 \rightarrow \text{N}_2\text{H}^+ + \text{H}$ rate decreased with

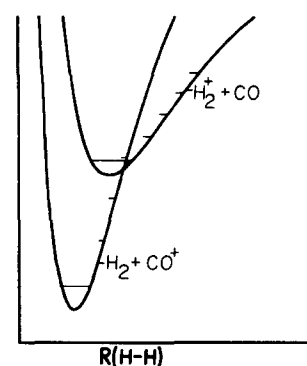


FIG. 2. Cut through $(\text{H}_2^+ + \text{CO})^+$ entrance channel at infinite reagent separation.

TABLE II. Estimated vibrational distributions.

Actual vibrational distribution	H_2^+ v nominal					D_2^+ v nominal				
	0	1	2	3	4	0	1	2	3	4
0	1	0.11	0.08	0.08	0.07	1	0.10	0.06	0.06	0.04
1		0.89	0.16	0.17	0.14		0.90	0.14	0.13	0.10
2			0.76	0.19	0.16			0.80	0.20	0.15
3				0.56	0.15				0.61	0.17
4					0.48					0.54

increasing collision energy with a concomitant increase in the charge transfer rate. They did not report the magnitude of the CT rate constant. Ryan⁹ studied the $(H_2 + N_2)^+$ system using a space charge trapping technique and obtained proton transfer rate constants in qualitative agreement with those of Bowers and Ellemann.⁸ Kim and Huntress¹⁰ reported an ICR study of $H_2^+ + N_2$ reactions in which the rate constant for N_2H^+ formation was given as $2.0 \times 10^{-9} \text{ cm}^3 \text{ molecule}^{-1} \text{ s}^{-1}$. No CT was observed under their conditions. The only dynamical studies of $(H_2 + N_2)^+$ have been crossed beam studies of $N_2^+ + H_2$ system.¹¹ The reaction was shown to proceed via a direct stripping type mechanism.

The rate constant for the process $H_2^+ + CO \rightarrow$ products was reported to be 2.95×10^{-9} by Ryan⁹ and $2.8 \times 10^{-9} \text{ cm}^3 \text{ molecule}^{-1} \text{ s}^{-1}$ by Huntress *et al.*¹⁰ Huntress *et al.* also report the branching between CT and HCO^+ production. Unlike $H_2^+ + N_2$, where no CT was observed in their experiment, the branching was 23% CT and 77% HCO^+ formation. In a crossed beam study, the charge reversed $CO^+ + D_2 \rightarrow DCO^+ + D$ reaction was shown to be direct with dynamics very nearly identical to those for $N_2^+ + H_2$.¹² Recently, a detailed crossed beam study of the $H_2^+ + CO \rightarrow HCO^+ + H$ reaction was carried out by Farrar *et al.*¹³ They found that the reaction was direct and, at low collision energies, most ($\sim 90\%$) of the available energy went into internal excitation of the HCO^+ product. As the collision energy was increased, the fraction of the total energy going to product internal excitation dropped to $\sim 50\%$. They attributed this to dissociation of the more highly excited product formed at high collision energy. The results were interpreted in light of the complex set of PES which were calculated by Vaz Pires *et al.*¹⁴

For $H_2^+ + O_2$, Huntress *et al.*¹⁰ studied the CT and PT reactions at thermal energies. They report a rate constant of $2.7 \times 10^{-9} \text{ cm}^3 \text{ molecule}^{-1} \text{ s}^{-1}$ for the sum of the two channels with 29% CT and 71% O_2H^+ formation. Again, the only dynamical study is of the $O_2^+ + H_2 \rightarrow O_2H^+ + H$ reaction.¹⁵ This reaction was found to proceed through a long lived complex mechanism at low energies, switching to a more direct stripping type mechanism as the collision energy is increased above 5 eV. It is quite doubtful that $O_2^+ + H_2$ and $H_2^+ + O_2$ would exhibit similar reaction dynamics since the energy difference between the two charge states is so large (3.35 eV).

This paper will focus on the dynamical implications

of the translational and vibrational energy dependence of proton and charge transfer in $H_2^+ + N_2$, CO , and O_2 . A simple model will be used to assess the relative importance of Franck-Condon factors, energy resonance and excited states on CT.

II. EXPERIMENTAL

The apparatus and experimental conditions used for these experiments are described in detail elsewhere.⁵ Briefly, we use photoionization to form H_2^+ in a known vibrational distribution. The estimated⁵ vibrational distributions for the photoionizing energies used are given in Table II. The ions produced in the radio frequency ion guide are accelerated, formed into a beam and guided through a scattering cell filled with the neutral reagent. The use of radio frequency ion optics assures 100% product collection efficiency and allows us to easily maintain a narrow ion beam kinetic energy spread. The ions are then mass analyzed by a quadrupole mass spectrometer (QPMS) and counted. By taking data as a function of both the accelerating voltage and the photon energy for H_2^+ production, we obtain two sets of relative cross sections; one as a function of collision energy and the other as a function of the vibrational state of H_2^+ .

Data analysis is relatively simple. Having obtained cross sections as a function of collision energy at fixed photon energy and as a function of vibrational state at fixed collision energy, the data is checked for internal consistency. For the $H_2^+ + H_2$ system,⁵ where the QPMS can be operated at low resolution and the transmissions of both reagent and product ions are $\sim 100\%$, the two types of measurements typically agree within 5%. In cases of discrepancy, the experiment in doubt was repeated and, thus, a complete set of vibrational and collision energy dependent cross sections were obtained.

For the systems under discussion ($H_2^+ + CO$, Ar , N_2 , O_2), a similar procedure is followed. Here, because of nonunit QPMS transmission resulting from the necessity of resolving the products of CT and PT, the scale of the raw cross sections is somewhat arbitrary, due to small differences in QPMS tuning and resolution from run to run. This requires that the measured cross sections be scaled using the measured collision energy dependence from the fixed vibrational state scans and vice versa, in order to obtain the experimental relative cross sections as a function of vibrational and collision energy.

These reactions ($H_2^+ + N_2$, CO, O_2) are much more sensitive than those of the $H_2^+ + H_2$ system to surface contamination in the final section of the ion guide, presumably due to the very low laboratory translational energies for products formed by light ion heavy target systems at thermal energy. In cases where data appeared to be bad because of the loss of low energy products, those runs were rejected in favor of data taken when the ion guides were freshly cleaned.

In order to assign absolute values to the cross sections, corrections must be made for the difference in QPMS transmission for various ions. This was done by lowering the QPMS resolution as far as possible, to approximately $M/\Delta M \sim 0.8$, to attain near 100 transmission for all ions. This resolution is still enough to separate the primary (H_2^+) and product (N_2H^+ , N_2^+) ions, but results in a single peak for the CT and PT products. The cross section for product formation as a function of collision energy measured under this condition is assumed to be the sum of the absolute cross sections for the two predominate product channels (photon and charge transfer). By comparing the known energy dependences of the two channels and the energy dependence of the low resolution measurement, we obtain the proper factor with which to scale our relative cross sections to obtain absolute cross sections.

After obtaining raw absolute cross sections, we then use our estimates of the actual vibrational state distributions present in our state selected H_2^+ beams to correct the raw experimental cross sections for vibrational dependence. This is done by starting with the cross sections for $v=0$ and working up to $v=4$, iteratively subtracting out the contributions from the lower vibrational states. This procedure gives our best estimates for the actual vibrational dependences. Any errors in our estimates of the vibrational distributions will propagate through the set of data. Because the estimated purity of the vibrational state selection is high for $v=0$ and $v=1$ and falls off to only $\sim 50\%$ for $v=4$, this error is small for $v=0, 1$, and 2 and gets worse for 3 and 4. Although it is impossible for us to give error bars here, it is very important to point out that all of the vibrational effects we report are present in the raw data, and are merely amplified by the unfolding process. Our estimates of vibrational state purity are necessarily upper bounds. This is because for want of a better assumption, we have assumed that *all* autoionization leaves ions in the highest possible vibrational states.⁵ To the degree which this is wrong, the actual vibrational state purity calculated at each photon energy is too high. The effect of the error is to underestimate the magnitudes of the various vibrational effects observed. Comparison of our data on $H_2^+ + Ar$ ⁶ with that of Koyano and Tanaka¹⁶ suggests that this may be true to a small extent, primarily with $v=4$. In order to allow recorection of the observed vibrational effects if we subsequently improve our estimates of the vibrational distributions, we present both corrected and raw cross sections.

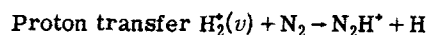
The estimated absolute error in these measurements is 25%. The relative error is estimated to be 5% at

the lowest collision energies for the proton transfer (e.g., N_2H^+ product) channels and at all energies for CT. The percent error in the proton transfer cross sections increases as the cross sections decrease and is estimated to be $\pm 10\%$ at the highest energies. For CT, there is an additional source of error caused by diffusion of the neutral scattering gas into the ion source. For $H_2^+ + O_2$ and $H_2^+ + CO$, the error is estimated to be less than 5%. For $H_2^+ + N_2$, this causes no error for $v=0$ but may introduce a 5% error for $V=1-4$. In addition, our correction of the cross sections for the H_2^+ vibrational state distribution possibly underestimates the magnitude of the vibrational effects especially for $v=3$ and 4 where the error may be as high as 20%.

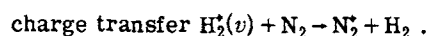
III. RESULTS

A. $H_2^+ + N_2$

Figure 3 shows our results for the vibrational and collision energy dependence of the two major reaction channels;



and



The analogous data for $D_2^+ + N_2$ is shown in Fig. 4. Table III contains the same cross sections as the two figures and, in addition, presents the raw data before the vibrational unfolding process.

The most striking feature of the data for $H_2^+(D_2^+) + N_2$ is the strong vibrational effect on CT. For $H_2^+ + N_2$, the cross section increases by about a factor of 6 when the ion is excited from $v=0$ to $v=1$. The cross section then decreases by $\sim 50\%$ going from $v=1$ to $v=2$ and again by

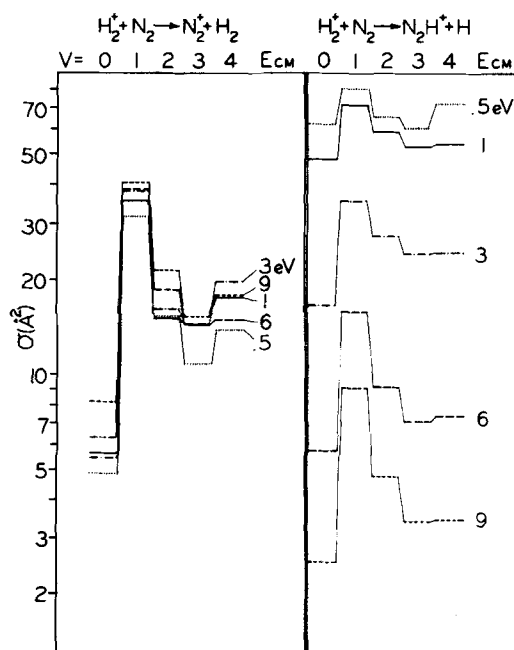


FIG. 3. Vibrational effects on $H_2^+ + N_2$ cross sections.

TABLE III. Raw and vibrationally corrected data for $H_2^+ + N_2$.

Reaction	$E_{c.m.}$	Corrected					Raw				
		$v=0$	1	2	3	4	$v=0$	1	2	3	4
$H_2^+ + N_2$, CT	0.5	4.86	31.7	15.3	10.8	13.8	4.86	28.7	17.1	14.7	15.4
	1	5.63	35.5	15.0	14.5	17.7	5.63	32.2	17.5	17.4	18.4
	3	5.45	38.0	16.2	14.5	18.8	5.45	34.4	18.8	18.1	19.5
	6	6.3	38.5	18.7	14.5	14.9	6.3	34.9	20.9	18.7	18.2
	9	8.23	40.7	21.5	15.3	17.9	8.23	37.1	23.5	20.2	20.6
$H_2^+ + N_2$, PT	0.5	62.0	80.5	65.5	60.2	72.0	62.0	78.5	67.6	64.8	69.7
	1	47.9	71.8	58.7	52.7	53.7	47.9	69.2	59.9	56.7	56.5
	3	16.6	35.1	27.5	24.2	24.4	16.6	33.1	27.8	26.1	25.8
	6	5.72	15.9	9.12	7.07	7.38	5.72	14.8	9.93	8.85	8.69
	9	2.52	9.10	4.75	3.39	3.44	2.52	8.37	5.27	4.55	4.37
$D_2^+ + N_2$, CT	0.5	3.38	29.1	19.5	29.4	26.5	3.38	26.5	19.9	25.8	25.4
	1	3.44	33.0	19.6	29.0	27.9	3.44	30.0	20.5	26.1	26.5
	3	3.96	35.7	22.1	28.9	28.5	3.96	32.5	22.9	26.9	27.5
	6	4.34	37.1	23.7	28.4	29.0	4.34	33.8	24.4	27.1	28.0
	9	5.29	37.0	25.0	32.5	32.6	5.29	33.8	25.5	29.9	30.9
$D_2^+ + N_2$, PT	0.5	75.6	80.2	79.1	76.3	73.5	75.6	79.7	79.0	77.3	73.3
	1	73.0	70.9	69.8	70.7	60.3	73.0	71.1	71.1	70.7	62.7
	3	16.1	28.4	26.9	28.1	26.8	16.1	27.2	26.5	27.2	26.4
	6	4.16	10.6	8.75	9.14	9.00	4.16	9.93	8.73	8.95	8.87
	9	1.57	3.82	3.72	3.76	3.65	1.57	3.50	2.81	3.43	3.43

about 30% from $v=2$ to 3 followed by a $\sim 25\%$ rise from 3 to 5.

For D_2^+ , the vibrational pattern for CT is quite different. The $D_2^+ v=0$ CT cross section is 25% lower than that for H_2^+ , but rises to approximately the same magnitude when the D_2^+ is in the $v=1$ state (factor of 9 jump). The decrease from $v=1$ to 2 is only $\sim 30\%$ and the cross section rises from 2 to 3 by $\sim 25\%$, followed by a slight decrease from $v=3$ to 4. The differences between H_2^+ and D_2^+ seen here are much larger than those for $H_2^+(D_2^+) + Ar$ presented in Ref. 6. As in all the cases of CT studied in our lab so far, there is very little cross sectional dependence with collision energy in the range between 0.5–9 eV.

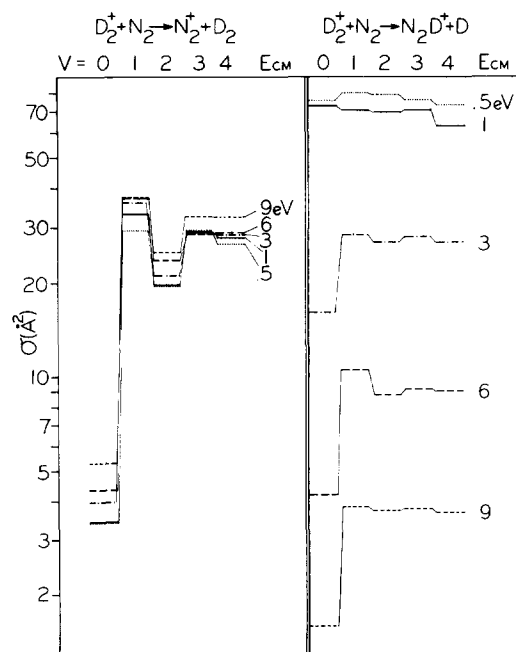
The PT cross sections show strong vibrational and collision energy dependence. The overall collision energy dependence for PT is a rapid drop from $\sim 70 \text{ \AA}^2$ at 0.5 eV to between 2 and 4 AA^2 at 9 eV. The cross sections at the lowest collision energy are about the same for H_2^+ and D_2^+ , which is what is expected from a Langevin type model. PT cross sections for both $H_2^+ + N_2$ and $D_2^+ + N_2$ fall off quite a bit faster than the Langevin type $E_{c.m.}^{-1/2}$ dependence which is thought to be common for exoergic ion-molecule reactions. Of the two, the D_2^+ PT cross section falls off faster so that at 9 eV it is $\sim 40\%$ lower than that for $H_2^+ (v=0)$.

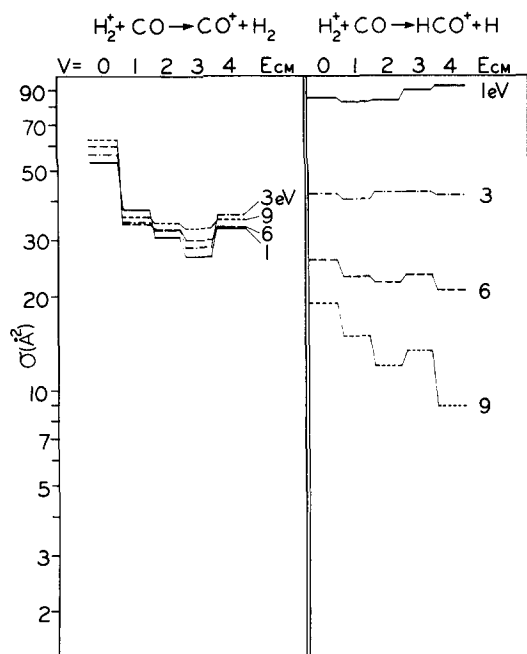
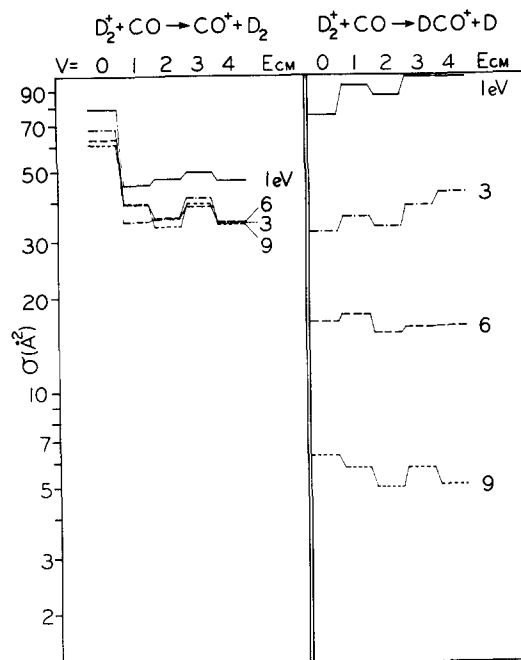
The vibrational effects on PT are quite complex, but a comparison between the effects for proton and charge transfer reveal a simple pattern for both H_2^+ and $D_2^+ + N_2$. At low collision energies, PT appears to be dominated by a mechanism which is relatively independent of vibrational state. As the collision energy increases, however, the vibrational effects for PT begin to mimic those for CT more and more, so that by 6 eV the vibrational effects for the two processes are

qualitatively identical. This same effect was observed in $H_2^+(D_2^+) + Ar$ PT.⁶

B. $H_2^+ + CO$

Figure 5 shows vibrational state dependent data for charge and proton transfer of H_2^+ with CO. The analogous data for $D_2^+ + CO$ is shown in Fig. 6. Both the raw and unfolded data for these systems is presented in Table IV. The most obvious effect of vibrational excitation

FIG. 4. Vibrational effects on $D_2^+ + N_2$ cross sections.

FIG. 5. Vibrational effects on $\text{H}_2^+ + \text{CO}$ cross sections.FIG. 6. Vibrational effects on $\text{D}_2^+ + \text{CO}$ cross sections.

in these systems is the large ($\sim 45\%$) drop in charge transfer cross section when the ion (H_2^+ or D_2^+) is excited from $v=0$ to $v=1$ with little change in cross section as the vibrational excitation is increased further.

For proton transfer, the H_2^+ and D_2^+ reactions again show similar vibrational effects, a small overall vibrational enhancement at low collision energy changing to vibrational inhibition at higher collision energy. The degree of enhancement at low energies is larger for D_2^+ than H_2^+ and is reflected in a lesser degree of vibrational inhibition at the higher energies. Again, there is virtually no collision energy dependence of the charge transfer reactions, while the proton transfer reaction cross sections decrease rapidly with increasing collision

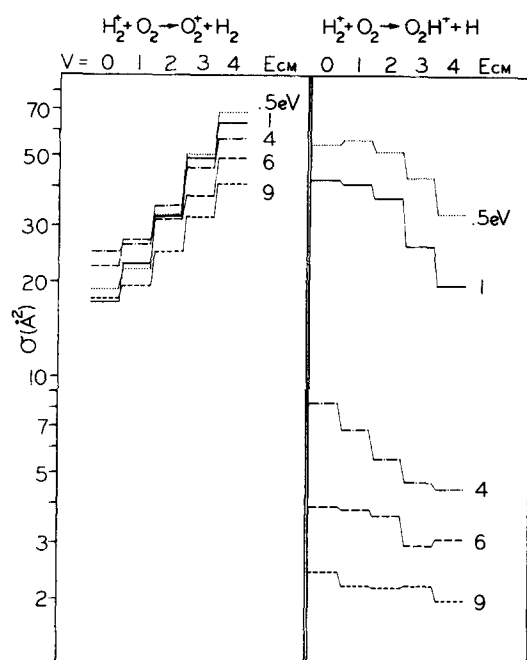
energy with the D_2^+ PT cross section falling off more rapidly than that for H_2^+ . One interesting point is that the magnitudes of the $\text{H}_2^+(\text{D}_2^+) + \text{CO}$ cross sections are $\sim 40\%$ – 50% larger than the corresponding $\text{H}_2^+(\text{D}_2^+) + \text{Ar}$, N_2 , and O_2 cross sections.

C. $\text{H}_2^+ + \text{O}_2$

Only the H_2^+ reactions were studied for this system. The CT and PT data are presented in Fig. 7 and Table V. $\text{H}_2^+ + \text{O}_2$ is unusual in that it is the only case studied so far in which the proton transfer reaction is inhibited by vibration (factor of ~ 2 drop going from $v=0$ – 4) at all collision energies. The CT cross sections show monotonic vibrational enhancement which also has not

TABLE IV. Raw and vibrationally corrected data for $\text{H}_2^+ + \text{CO}$.

Reaction	$E_{\text{c.m.}}$	Corrected					Raw				
		$v=0$	1	2	3	4	$v=0$	1	2	3	4
$\text{H}_2^+ + \text{CO}$, CT	1	53.2	37.4	30.7	26.5	32.7	53.2	39.1	33.6	31.3	33.5
	3	56.3	34.3	32.2	28.5	36.1	56.3	36.7	34.5	32.4	35.5
	6	59.9	33.9	32.5	30.1	33.9	59.9	36.8	34.9	33.6	34.9
	9	62.7	35.6	34.1	32.7	34.9	62.7	38.6	36.6	35.8	36.5
$\text{H}_2^+ + \text{CO}$, PT	1	85.1	82.4	83.8	91.5	39.0	85.1	82.7	83.7	87.9	89.3
	3	42.4	40.6	42.7	42.9	42.1	42.4	20.8	42.3	42.4	42.1
	6	26.0	23.1	22.1	23.3	21.0	26.0	23.4	22.6	23.2	22.2
	9	19.0	14.9	12.0	13.4	8.9	19.0	15.4	13.0	13.8	11.6
$\text{D}_2^+ + \text{CO}$, CT	1	79.0	45.2	47.0	49.5	46.7	79.0	48.6	48.7	50.2	45.7
	3	68.2	34.6	35.1	41.3	34.4	68.2	38.0	37.0	40.8	34.7
	6	63.1	39.4	35.5	38.7	34.6	63.1	41.8	37.7	39.6	34.9
	9	61.0	39.6	33.4	39.5	34.1	61.0	41.7	35.9	39.6	34.4
$\text{D}_2^+ + \text{CO}$, PT	1	74.8	29.5	86.2	98.4	97.8	74.8	90.7	86.4	93.8	92.7
	3	31.9	35.6	33.1	38.6	42.3	31.9	35.2	33.4	36.7	38.4
	6	16.7	17.5	15.3	16.1	16.2	16.7	17.4	15.7	16.2	15.7
	9	6.27	5.47	4.98	5.76	5.10	6.27	5.79	5.16	5.63	5.11

FIG. 7. Vibrational effects on H_2^+ cross sections.

been observed before. The increase in CT is almost a factor of 2.5 going from $v=0-4$. The collisional energy dependence of the CT and PT cross sections are similar to all other systems investigated.

IV. DISCUSSION

A. $H_2 + N_2$

The size and lack of collision energy dependence for charge transfer in this and all other systems investigated implies that the probability of charge transfer becomes substantial at a relatively large intermolecular distance where the charge-induced-dipole interaction is small compared to the collision energy. General features of charge transfer in $H_2^+ + Ar$ are similar to those observed in this system. The similarity is expected since both systems have similar avoided crossings in the collision entrance channels, mainly due to the similarity in the energetics, which allow vibration of the reagents to cause transitions from one charge

state to the other (e.g., $H_2^+ + N_2 \rightleftharpoons H_2 + N_2^+$). Charge hopping for $H_2^+ + Ar$ is predicted⁴ to start at reagent separations of $\sim 4-5$ Å, which is consistent with the observed⁶ ~ 40 Å² CT cross sections. Since the magnitude of the CT cross sections observed (Figs. 3 and 4) for $H_2^+(D_2^+) + N_2$ [except for $H_2^+(D_2^+) v=0$], is also ~ 40 Å², the mixing for N_2 must also start to occur at ranges of $4-5$ Å.

The actual patterns of vibrational dependence for H_2^+ and D_2^+ charge transfer with N_2 are quite different from each other and from those for CT with argon. This is simply due to differences in the energy matchings and overlaps of wave functions between the initial state and available final states. The energetics of CT for H_2^+ and D_2^+ with N_2 are shown in Figs. 8 and 9. For both H_2^+ and D_2^+ in the $v=0$ state, charge transfer is endoergic and requires substantial translational-to-internal energy conversion. This requires "hard" collisions (i.e., small impact parameter) and results in small $H_2^+(D_2^+) v=0$ CT cross sections (~ 7 Å²). The same effect is observed for $H_2^+(D_2^+) + Ar$, where the endoergic is even higher (0.31 eV) and the cross sections only $\sim 2-3$ Å². All the other $H_2^+(D_2^+) + N_2$ initial states have exoergic CT final states available for charge transfer. The strong variation of the CT cross sections with ion vibrational level is due to both energy gap and Franck-Condon factors and will be discussed later.

For H_2^+ and D_2^+ proton transfer with N_2 (Figs. 3 and 4), vibrational excitation of the ion has little effect on reactivity at low collision energy. As the energy increases, however, the proton transfer vibrational dependence begins to mirror that for charge transfer. This implies that the same dynamical effects responsible for increasing CT cross sections, i.e., favorable energy resonance and "Franck-Condon" factors which result in large probability of charge hopping (strong mixing) between the two reagent states, also greatly increase the probability of subsequent proton transfer. The same strong coupling between charge hopping and proton transfer has been observed for the $H_2^+(D_2^+) + Ar$ system, but not for the other systems we have studied ($H_2^+ + H_2$, CO, O₂). The similarity of the reaction dynamics for $H_2^+ + Ar$ and N_2 must be due largely to the similarity of the entrance channel avoided crossings which occur for both systems, since one would expect

TABLE V. Raw and vibrationally corrected data for $H_2^+ + O_2$.

Reaction	E_{cm}	Corrected					Raw				
		$v=0$	1	2	3	4	$v=0$	1	2	3	4
$H_2^+ + O_2$, CT	0.5	18.9	21.9	32.5	50.5	68.6	18.9	21.6	29.7	39.7	50.1
	1	17.2	22.8	32.2	49.2	63.6	17.2	22.2	29.5	38.9	47.4
	4	24.9	26.2	34.8	45.9	56.7	24.9	26.1	32.6	38.8	45.1
	6	22.4	27.1	31.5	37.4	49.1	22.4	26.6	30.1	33.3	39.6
	9	17.7	19.4	24.9	32.0	40.9	17.7	19.2	23.4	27.4	32.4
$H_2^+ + O_2$, PT	0.5	54.8	56.2	51.6	42.9	32.9	54.8	56.0	52.6	47.8	42.2
	1	42.3	40.8	36.9	26.1	19.6	42.3	41.1	38.0	32.0	27.9
	4	8.33	6.87	5.56	4.70	4.48	8.33	7.03	5.99	5.52	5.29
	6	3.94	3.84	3.67	2.96	3.10	3.94	3.85	3.72	3.32	3.33
	9	2.45	2.22	2.18	2.22	1.99	2.45	2.24	2.21	2.23	2.12

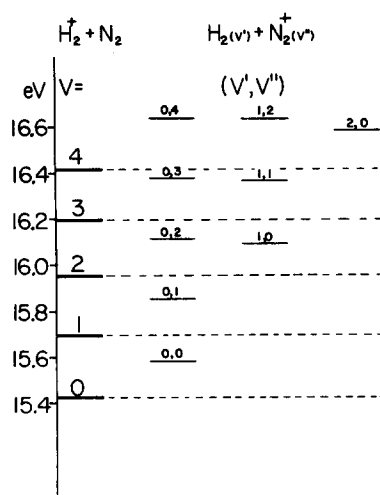


FIG. 8. Energetics for $\text{H}_2^+ + \text{N}_2$ CT, showing reagent total energies (left) and various product state energies.

that the potential energy surfaces for the two systems would be quite different at close range. This points out how strongly entrance channel avoided crossings can affect ion-molecule reaction dynamics.

The mechanism by which high charge hopping probability is reflected in increased proton transfer probability is unclear. One possibility is that in the repeated charge hops which occur as the reagents approach, the system may end up in favorable geometric configuration between reagents or that transfer of some translational energy to vibrational energy may occur, with concomitant reduction in relative velocity, thus increasing the proton transfer cross section (Figs. 3 and 4).

One difference between the $\text{H}_2^+ + \text{Ar}$ and $\text{H}_2^+ + \text{N}_2$ systems is in the collision energy dependence of CT. For $\text{H}_2^+(\text{D}_2^+) v=0 + \text{Ar}$ charge transfer, peaks were observed in the collision energy dependence.⁶ We were able to use an energy gap model of Massey¹⁷ to fit the peaks. The assumption was that the peaks were due to for-

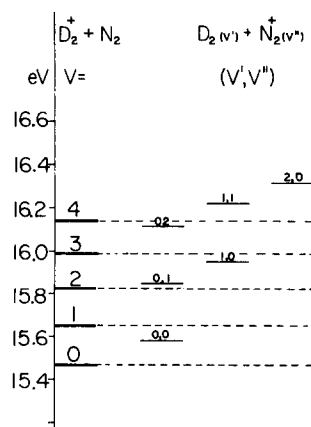


FIG. 9. Energetics for $\text{D}_2^+ + \text{N}_2$ CT, showing reagent total energies (left) and various product state energies.

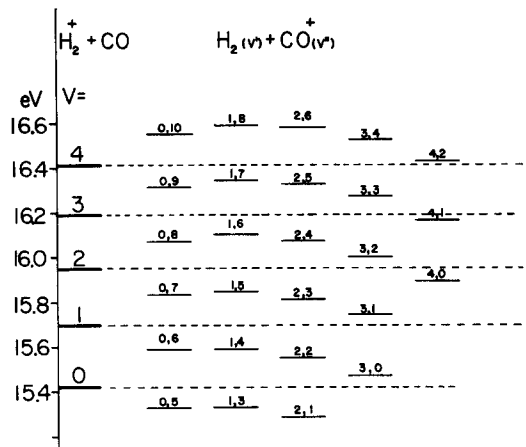


FIG. 10. Energetics for $\text{H}_2^+ + \text{CO}$ CT, showing reagent total energies (left) and various product state energies.

mation of two different electronic states of $\text{Ar}^*(^2P_{1/2,3/2})$, both of them endoergic. For $\text{H}_2^+(\text{D}_2^+) v=0$ CT with N_2 , although there are several low lying endoergic channels, no structure was observed. Added N_2 rotational degrees of freedom might smear out any possible structure in this system or it could be that the probability of forming the vibrationally excited product states is so small that they don't show up as peaks.

For both $\text{H}_2^+ + \text{Ar}$ and N_2 , the detailed mechanism for proton transfer is worth pursuing further theoretically, perhaps using the trajectory surface hopping model¹⁸ or a semiclassical variation thereof.¹⁹

B. $\text{H}_2^+ + \text{CO}$

This system is quite different from $\text{H}_2^+ + \text{N}_2$. Here, charge transfer from all H_2^+ initial vibrational states is at least 1.4 eV exoergic. The large difference in ionization potential between H_2 and CO also changes the nature of the avoided crossing which occurs in the entrance channel, as Figs. 1 and 2 show. While vibrational motion still couples the two reagent charge states ($\text{H}_2^+ + \text{CO}$, $\text{H}_2 + \text{CO}^+$), the stronger coupling is to high vibrational levels of the $\text{H}_2 + \text{CO}^+$ system, and charge transfer back is less likely. In $\text{H}_2^+ + \text{H}_2$, $\text{H}_2^+ + \text{Ar}$, and $\text{H}_2^+ + \text{N}_2$, the initial charge state (e.g., $\text{H}_2^+ + \text{Ar}$) correlates directly to the proton transfer product. The other reagent charge state ($\text{H}_2 + \text{Ar}^+$), at least in a diabatic picture, can only scatter nonreactively. In $\text{H}_2^+ + \text{CO}$, neither the $\text{H}_2 + \text{CO}^+ [^2A_1(1)]$ state of H_2CO^+ , nor the $\text{H}_2^+ + \text{CO} [^2A_1(2)]$ state correlates to $\text{HCO}^+ + \text{H}$. Rather, it is the X^2B_2 ground state of H_2CO^+ which correlates to the proton transfer product.^{13,14}

There are a number of possible avoided crossings which allow proton and charge transfer to occur for $\text{H}_2^+ + \text{CO}$. Vibrational motion at the seam in the entrance channel (Fig. 2) discussed above can couple $\text{H}_2^+ + \text{CO} [^2A_1(2)]$ and $\text{H}_2 + \text{CO}^+ [^2A_1(1)]$. Calculations by Vaz Pires *et al.*,¹⁴ show that the X^2B_2 state crosses both of the 2A_1 states, and in low symmetry collisions may cause not only charge transfer [$^2A_1(2) \rightarrow ^2A_1(1)$], but also may lead to proton transfer [$^2A_1(2) \rightarrow X^2B_2$].

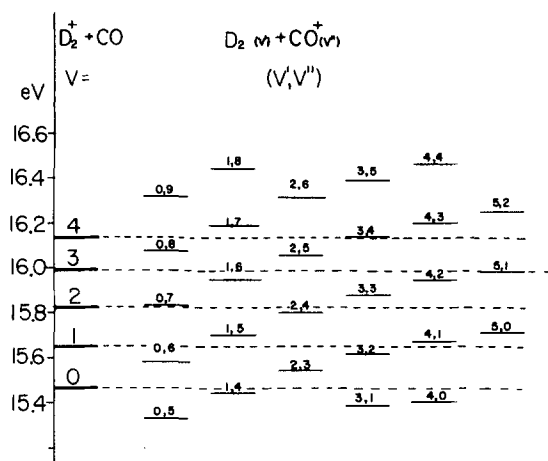


FIG. 11. Energetics for $D_2^+ + CO$ CT, showing reagent total energies (left) and various product state energies.

Crossing of these seams, however, is brought about by relative motion of the reagents. Needless to say, the very complicated system of potential surfaces and crossing seams makes it difficult to draw dynamical conclusions from the vibrational and collision energy dependences we observe.

The magnitudes of both the proton transfer and charge transfer channels of the $H_2^+(D_2^+) + CO$ reaction are 40%–50% larger than those for $H_2^+ + Ar$ or N_2 . This is possibly due to the additional attractive ion-permanent dipole term in the interaction potential,²⁰ or because CT back to the reagent charge state is less likely for $H_2^+ + CO$ than for N_2 or Ar .

The relatively large charge transfer cross sections and the lack of collision energy independence again indicate that CT occurs by a long range process. The fact that there is no appreciable collision energy dependence, yet the vibrational dependence is quite pronounced, suggests that the coupling between the charge states is more vibrational than translational and occurs via vibration through the seam between the two 2A_2 surfaces in the collision entrance channel. If the primary CT pathway was via the X^2B_1 state, then one would expect some collision energy dependence, since the motion through this seam is translational.^{13,14} The CT cross section is observed to drop by ~45% when the ion is excited from $v=0$ to $v=1$ with relatively little effect from subsequent vibrational excitation. This may be due to the fact that, at long range, the outer classical turning point for the $v=0$ vibration occurs just where the $H_2^+ + CO$ and $CO^+ + H_2$ surfaces cross. This might be expected to increase the $H_2^+(v=0) + CO$ charge transfer probability.

The vibrational dependence of the proton transfer is quite weak and apparently patternless for $H_2^+ + CO$. This is in strong contrast to the cases of $H_2^+ + Ar$ and N_2 . However, the lack of strong vibrational effects is not too surprising in light of the energetics involved. As H_2^+ and CO approach each other in the entrance channel, most of the time the system will vibrate through the avoided crossing between the $H_2^+ + CO$ and $CO^+ + H_2$ potential surfaces and charge transfer to highly excited $CO^+ + H_2$ states containing as much as 1.4 eV vibrational energy. The effect of the relatively small amount of initial vibrational excitation would be expected to be fairly insignificant. This is in contrast to the cases of

TABLE VI. Experimental and calculated vibrational dependence of $H_2^+ + Ar$ charge transfer.

$H_2^+ + Ar$								
		Best fit		Without H_2FC 's		Without Ar stat. factors		Without ΔE law
$v =$	Exptl.	$K=4$ $E_0=0.5$	2 0.3	4 0.5	2 0.3	4 0.5	2 0.3	1 1000
0	0.04	0.03	0.06	0.05	0.09	0.03	0.05	1.00
1	0.46	0.51	0.67	0.42	0.58	0.40	0.52	0.94
2	1.00	1.00	1.00	0.75	0.84	1.00	1.00	0.89
3	0.67	0.56	0.41	0.79	0.84	0.57	0.41	0.84
4	0.54	0.40	0.28	1.00	1.00	0.39	0.27	0.79

$D_2^+ + Ar$								
		Best fit		Without D_2FC 's		Without Ar stat. factors		Without ΔE law
$v =$	Exptl.	$K=4$ $E_0=0.5$	2 0.3	4 0.5	2 0.3	4 0.5	2 0.3	1 1000
0	0.05	0.03	0.06	0.06	0.10	0.02	0.05	1.00
1	0.41	0.30	0.41	0.26	0.36	0.24	0.35	0.99
2	1.00	0.93	1.00	0.61	0.70	0.80	0.95	0.99
3	0.88	1.00	0.90	0.76	0.81	1.00	1.00	0.99
4	0.70	0.60	0.51	1.00	1.00	0.66	0.55	0.86

TABLE VII. Experimental and calculated vibrational effects for $H_2^+ + N_2$ charge transfer.

$H_2^+ + N_2$								
$v =$	Exptl.	Best fit		Without $H_2FC's$		Without $N_2FC's$		Without ΔE law
		$K=4$	2	4	2	4	2	1
		$E_0=0.5$	0.3	0.5	0.3	0.5	0.3	1000
0	0.20	0.20	0.27	0.24	0.37	0.08	0.13	1.00
1	1.00	1.00	1.00	0.70	0.76	0.52	0.61	0.94
2	0.53	0.81	0.63	0.70	0.73	0.85	0.89	0.89
3	0.38	0.48	0.31	1.00	1.00	0.92	0.90	0.84
4	0.44	0.52	0.47	0.88	0.96	1.00	1.00	0.79

$D_2^+ + N_2$								
$v =$	Exptl.	Best fit		Without $D_2FC's$		Without $N_2FC's$		Without ΔE law
		$K=4$	2	4	2	4	2	1
		$E_0=0.5$	0.3	0.5	0.3	0.5	0.3	1000
0	0.11	0.14	0.22	0.29	0.40	0.07	0.11	1.00
1	1.00	0.76	0.88	0.65	0.74	0.41	0.52	0.99
2	0.62	1.00	1.00	0.72	0.77	0.87	0.99	0.99
3	0.81	0.78	0.66	1.00	1.00	0.93	0.95	0.99
4	0.80	0.57	0.52	0.94	0.91	0.00	1.00	0.86

$H_2^+ + Ar$ and N_2 , where charge transfer and surface hopping are energetically impossible for the ground vibrational state and the initial vibrational excitation was found to be very important in determining the cross sections for both proton and charge transfer.

C. $H_2^+ + O_2$

The strong monotonic vibrational enhancement for charge transfer and monotonic vibrational inhibition for proton transfer is a unique feature for this system. Because the IP of O_2 is 3.35 eV less than that of H_2 , crossings occur between the $H_2^+ + O_2$ surface and the high vibrational levels of the $O_2^+ + H_2$ system. The strong vibrational enhancement for CT is probably mainly due to the increased number of $O_2^+ + H_2$ product states available for near resonant CT as the energy of the $H_2^+ + O_2$ initial state is increased. The vibrational enhancement seen here is reproduced by the model calculation which will be described later.

The fact that the proton and charge transfer channels show roughly equal but opposite vibrational effects, suggests that maybe competition is occurring between these two channels. Unlike the cases of $H_2^+ + N_2$ and $H_2^+ + Ar$, when charge transfer occurs in the entrance channel of an $H_2^+ + O_2$ collision, the possibility of vibrational relaxation during the collision makes charge transfer back to the initial reagent state unlikely, similar to the exoergic charge transfer of $H_2^+ + CO$ discussed earlier. The apparent competition suggests that those $H_2^+ + O_2$ collisions which transfer to the $O_2^+ + H_2$ surface at the entrance channel avoided crossing simply end up as $O_2^+ + H_2$ charge transfer products; proton transfer results mainly from a fraction of those collisions which do not charge transfer early in the collision. Due to the lack of any detailed information about the nature of the $H_2O_2^+$

potential surfaces, this suggestion is, of course, speculative.

D. A simple model of charge transfer

As noted in the introduction, some question exists of what effect energy resonance and Franck-Condon factors have on the charge transfer process. The consensus from many studies performed of CT, where emission from excited products is observed,^{21,22} appears to be that energy resonance effects are important at all collision energies and that Franck-Condon effects are important at high collision energy where the collision time is short with respect to a vibrational period, and less so at lower collision energies. Effects like curve crossings appear to perturb the distribution of final states significantly.²² The 0.5–10 eV collision energy of our experiments in the range, where the collision time is about two to ten vibrational periods.

While it is true that looking at the product state distribution is a more direct method of observing how various dynamical factors influence charge transfer, modeling of the total CT cross section out of various initial vibrational states provides some additional information, since the pattern of Franck-Condon overlaps and energy gaps for forming different product states is different for each initial vibrational state of the ion.

A simple model was chosen to attempt to fit the observed vibrational dependences of the charge transfer cross sections. Basically, we assume that the charge transfer probability from an initial $H_2^+(v) + M(v=0)$ state to a given $H_2(v') + M^+(v')$ final state is proportional to the product of the Franck-Condon (FC) factors for neutralizing $H_2^+ [H_2^+(v) - H_2(v')]$, and for ionizing the neutral $[M(v=0) - M^+(v')]$, times a factor $f(\Delta E)$, which is

TABLE VIII. Experimental and calculated vibrational dependence for $H_2^+ + CO$ charge transfer.

$H_2^+ + CO$								
		Best fit		Without H_2FC 's		Without COFC's		Without ΔE law
$v =$	Exptl.	$K=4$ $E_0=0.5$	2 0.3	4 0.5	2 0.3	4 0.5	2 0.3	1 1000
0	1.00	1.00	1.00	0.82	0.81	1.00	1.00	1.00
1	0.57	0.47	0.53	0.73	0.66	0.75	0.72	0.94
2	0.54	0.25	0.21	0.93	0.89	0.68	0.63	0.89
3	0.50	0.30	0.32	0.86	0.82	0.65	0.62	0.84
4	0.56	0.29	0.36	1.00	1.00	0.62	0.60	0.79

$D_2^+ + CO$								
		Best fit		Without D_2FC 's		Without COFC's		Without ΔE law
$v =$	Exptl.	$K=4$ $E_0=0.5$	2 0.3	4 0.5	2 0.3	4 0.5	2 0.3	1 1000
0	1.00	1.00	1.00	0.85	0.82	1.00	1.00	1.00
1	0.62	0.72	0.92	0.94	0.82	0.75	0.76	0.99
2	0.56	0.30	0.34	0.85	0.80	0.61	0.59	0.99
3	0.61	0.34	0.39	1.00	1.00	0.57	0.55	0.99
4	0.55	0.26	0.33	0.89	0.86	0.51	0.48	0.86

determined by the energy gap. The total charge transfer probability from an initial state is then the sum of the probability to all the possible final states. Thus,

$$P[H_2^+(v) + M] = \sum_v \sum_{v'} FC[H_2(v', v)] FC[M(v'')] f(\Delta E).$$

The Franck-Condon factors for neutralizing H_2^+ were calculated by Flannery *et al.*²³ Those for D_2^+ were calculated by Dr. Dennis Trevor of our laboratory using RKR-Morse potentials to calculate the D_2 and D_2^+ wave functions. The Franck-Condon factors for ionizing N_2 , CO , and O_2 are from Gardner and Samson,²⁴ except that, in cases where the Franck-Condon factor is zero for a given transition, the calculation used a value of 10^{-5} just to allow those states to contribute slightly. Several types of energy gap laws were tried. The best overall seemed to be an exponential form:

$$f(\Delta E) = \exp(-\Delta E/E_0),$$

where ΔE is the energy difference between initial and final states and E_0 is a parameter which gives the range of the exponential function. The calculation consists of varying E_0 and calculating the total charge transfer probability for each initial $H_2^+(D_2^+)$ vibrational state, normalized to one for whatever state has the largest probability.

The simplest system $H_2^+ + Ar$ was used as a test case. For Ar, instead of Franck-Condon factors, the statistical factors for forming Ar^+ in the $^2P_{3/2}$ or $^2P_{1/2}$ states were used. It was found to be impossible to reproduce the observed 0.04:0.46:1 ratio of the CT cross sections for $H_2^+ v=0, 1$, and 2 unless the energy gap law was changed to make the exponential fall off faster for endoergic channels than for exoergic ones. The form used was

$$f(\Delta E) = \exp(-K\Delta E/E_0),$$

where K is 1.0 for exoergic channels, and larger than 1.0 for endoergic channels. With this addition, it was possible to obtain qualitative fits to the data for all the CT reactions studied. Results are shown in Tables VI-IX. The experimental vibrationally dependent CT probability (normalized to one) and the calculated CT probability for two different sets of K and E_0 parameters are included for comparison. While it is possible to slightly improve the fit for a given reaction, for these two sets $K=4$, $E_0=0.5$ and $K=2$, $E_0=0.3$ provide the best qualitative overall fit. The model reproduces the increases and decreases in CT probability and the peak vibrational states, with the exception of the $D_2^+ + N_2$ case where the calculated peak is at $v=3$ instead of $v=2$. Quantitatively, the model tends to overestimate the magnitudes of the vibrational effects. In order to assess the importance of the Franck-Condon factors, calculations were performed for the best fit K and E_0 , first leaving out the H_2 Franck-Condon factors and then the Franck-Condon factors for the other reagent. The final column in the tables gives the result when $K=1$ and $E_0=1000$, which essentially removes the dependence of charge transfer probability on the energy gap. Leaving out any of these factors was found to completely destroy the agreement with experiment.

The fact that the model, which basically ignores any dynamical effects on CT, agrees reasonably well with the experiment, is further support for the idea that CT occurs at large reagent separation. Not surprisingly, the model suggests that the importance of a particular CT channel decreases rapidly as the energy gap between the reagent state and the particular product state increases. The model also requires that, for a given energy gap, endoergic CT channels are much less im-

TABLE IX. Experimental and calculated vibrational dependence of $\text{H}_2^+ + \text{O}_2$ charge transfer.

$v =$	Exptl.	$\text{H}_2^+ + \text{O}_2$								
		Best fit		Including α state		Without $\text{H}_2\text{FC}'\text{s}$		Without $\text{D}_2\text{FC}'\text{s}$		Without ΔE law
		$K=4$ $E_0=0.5$	2	4	2	4	2	4	2	
0	0.46	0.26	0.08	0.15	0.04	0.89	0.92	1.00	1.00	1.00
1	0.55	0.46	0.26	0.28	0.11	0.95	0.98	0.94	0.95	0.94
2	0.64	0.68	0.52	0.43	0.28	1.00	1.00	0.89	0.91	0.89
3	0.76	0.87	0.72	0.66	0.58	0.95	0.88	0.84	0.84	0.84
4	1.00	1.00	1.00	1.00	1.00	0.79	0.66	0.79	0.80	0.79

portant than exoergic ones, although the translational energy is more than enough to compensate for the endoergicity. Somewhat surprisingly, it appears that Franck-Condon factors are very important in determining CT probability, in spite of the fact that the collisions are slow with respect to the vibrational period of the molecules.

N_2^+ , CO^+ , and O_2^+ all have low lying electronic states (Table I). For N_2^+ and CO^+ , these are high enough in energy so that, at least in the model calculations, they do not contribute more than a few percent to the CT probability. This is borne out experimentally by the fact that the CT cross sections do not change significantly when the collision energy is raised to the point where CT to the excited state channel is energetically possible. For $\text{H}_2^+ + \text{O}_2$, the model shows some dependence on whether or not the first excited state is included. Inclusion (see Table VIII) increases the vibrational dependence of the CT cross section substantially. But experimentally, it again appears that CT to the $a^4\Pi_u$ state of O_2^+ cannot be very important since CT has very little collision energy dependence, actually dropping off slightly with increased collision energy.

V. CONCLUSIONS

Comparison of the strikingly different vibrational and collision energy dependences for $\text{H}_2^+ + \text{Ar}$, N_2 , CO , and O_2 reactions allows us to examine the changes in charge and proton transfer dynamics brought about by the differences in energetics for the four systems. Charge transfer, at least where exoergic, is observed to be a long range, collision energy independent process. Modeling of charge transfer probabilities shows that both energy resonance and Franck-Condon effects are quite important.

The similarities between $\text{H}_2^+ + \text{Ar}$ and $\text{H}_2^+ + \text{N}_2$ reactions demonstrates that they occur by very similar mechanisms. In both cases, charge and proton transfer are seen to be strongly coupled at high collision energies and probably involve vibrationally induced charge and surface hopping transitions in the collision entrance channels.

For $\text{H}_2^+ + \text{CO}$ and $\text{H}_2^+ + \text{O}_2$, the linkage between proton and charge transfer is not as clear. For $\text{H}_2^+ + \text{O}_2$, PT and CT show opposite vibrational dependences which

may indicate a form of competition between the two channels. The lack of collision energy dependence and stronger vibrational dependence of CT of these systems studied suggests that CT is induced vibrationally rather than translationally as was suggested by potential energy surface calculations of similar systems.

ACKNOWLEDGMENTS

This work was supported by the Director, Office of Energy Research, Office of Basic Energy Sciences, Chemical Sciences Division of the U.S. Department of Energy under Contract DE-AC03-76SF00098.

- ¹D. S. Perry, J. C. Polanyi, and C. W. Wilson, Jr., *Chem. Phys.* **3**, 317 (1974); J. C. Polanyi and N. Sathyamurthy, *ibid.* **33**, 287 (1978); **37**, 259 (1979); A. M. G. Ding, L. J. Kirsh, D. S. Perry, J. C. Polanyi, and J. L. Schreiber, *Faraday Discuss. Chem. Soc.* **55**, 252 (1973).
- ²J. G. Pruett, F. R. Grabner, and P. R. Brooks, *J. Chem. Phys.* **63**, 1173 (1975); H. H. Disper, M. W. Geis, and P. R. Brooks, *ibid.* **70**, 5317 (1979); D. J. Douglas, J. C. Polanyi, and J. J. Sloan, *Chem. Phys.* **13**, 15 (1976); A. Gupta, D. S. Perry, and R. N. Zare, *J. Chem. Phys.* **72**, 6250 (1980).
- ³J. R. Krenos, K. K. Lehman, J. C. Tully, P. M. Hierl, and G. P. Smith, *Chem. Phys.* **16**, 109 (1976); J. R. Stine, and J. T. Muckerman, *J. Chem. Phys.* **68**, 185 (1978).
- ⁴S. Chapman and R. K. Preston, *J. Chem. Phys.* **60**, 650 (1974); M. Baer and J. A. Beswick, *Phys. Rev. A* **19**, 1559 (1979).
- ⁵Scott L. Anderson, F. A. Houle, D. Gerlich, and Y. T. Lee, *J. Chem. Phys.* **75**, 2153 (1981).
- ⁶F. A. Houle, S. L. Anderson, D. Gerlich, T. Turner, and Y. T. Lee, *Chem. Phys. Lett.* **82**, 392 (1981); *J. Chem. Phys.* (in preparation).
- ⁷Ray Walder and J. L. Franklin, *Int. J. Mass Spectrom. Ion Phys.* **36**, 85 (1980); K. P. Huber and G. Herzberg, *Constants of Diatomic Molecules* (Van Nostrand Reinhold, New York, 1979).
- ⁸M. T. Bowers, D. D. Elleman, and J. King, Jr., *J. Chem. Phys.* **50**, 1840 (1969); M. T. Bowers and D. D. Elleman, *ibid.* **51**, 4606 (1969).
- ⁹K. R. Ryan, *J. Chem. Phys.* **61**, 1559 (1974).
- ¹⁰J. K. Kim and W. T. Huntress, Jr., *J. Chem. Phys.* **62**, 2820 (1975).
- ¹¹Z. Herman, J. Kerstetter, T. Rose and R. Wolfgang, *Discuss. Faraday Soc.* **44**, 123 (1967); *J. Chem. Phys.* **46**, 2844 (1967); W. R. Gentry, E. A. Gislason, B. H. Mahan,

- and C. W. Tsao, *ibid.* **49**, 3058 (1968).
- ¹²J. Kerstetter and R. Wolfgang, *J. Chem. Phys.* **53**, 3765 (1970).
- ¹³R. M. Bilotta, F. N. Pruening, and J. M. Farrar, *J. Chem. Phys.* **72**, 1583 (1980).
- ¹⁴M. Vaz Pires, C. Galloy, and J. C. Lorquet, *J. Chem. Phys.* **69**, 3242 (1978).
- ¹⁵M. H. Chiang, E. A. Gislason, B. H. Mahan, C. W. Tsao, and A. S. Werner, *J. Phys. Chem.* **75**, 1426 (1971).
- ¹⁶I. Koyano and K. Tanaka, *J. Chem. Phys.* **72**, 4858 (1980).
- ¹⁷H. W. S. Massey and E. H. S. Burhop, *Electronic and Ionic Impact Phenomena* (Oxford, New York, 1952), p. 478.
- ¹⁸J. C. Tully, in *Dynamics of Molecular Collisions*, Part B, edited by W. H. Miller (Plenum, New York, 1976), p. 217.
- ¹⁹W. H. Miller and T. F. George, *J. Chem. Phys.* **56**, 5637 (1972).
- ²⁰See, e.g., M. T. Bowers and T. Su, *Adv. Electron. Electron Phys.* **34**, 246 (1973).
- ²¹A good review is found in M. Vaz Pires, C. Galloy, and J. C. Lorquet, *J. Chem. Phys.* **69**, 234 (1978).
- ²²T. R. Govers, M. Gerand, G. Marclaire, and R. Marz, *Chem. Phys.* **23**, 411 (1977).
- ²³M. R. Flannery, H. Tai, and D. L. Albritton, *At. Data Nucl. Data Tables* **20**, 563 (1977).
- ²⁴J. L. Gardner and J. A. R. Samson, *J. Electron. Spectrosc.* **13**, 7 (1978).